

# COMPARISON BETWEEN MEASURED AND COMPUTED TEMPERATURES OF THE INTERNAL HIGH ENERGY BEAM DUMP IN THE CERN SPS

G. Steele, F. Padeloup, R. Folch, V. Kain, I. V. Leitao, R. Losito, C. Maglioni, A. Perillo-Marccone, F. Velotti, CERN, Geneva, Switzerland

## Abstract

The SPS high energy internal dump (TIDVG) is designed to receive beam dumps from 102.2 to 450 GeV. The absorbing core is composed of 2.5 m graphite, followed by 1.0 m of aluminium, then 0.5 m of copper and 0.3 m of tungsten, all of which is surrounded by a water cooled copper jacket. An inspection during Long Shutdown 1 (LS1) revealed significant beam induced damage to the Al section of the dump block. Temperature sensors were installed to monitor the new dump replacing the damaged one. This paper summarises the correlation between the temperature measured as a function of the energy deposited and the corresponding temperatures computed in a numerical model combining FLUKA and ANSYS simulations. The goal of this study is the assessment of the thermal contact quality between the beam absorbing blocks and the copper jacket, by analysing the cooling times observed from the measurements and from the thermo-mechanical simulations. This paper presents an improved method to estimate the efficiency and long term reliability of the cooling of this type of design, with the view of optimising the performance of future dump versions.

## INTRODUCTION

The Target Internal Dump Vertical Graphite (TIDVG) device is used as a high energy (102.2 to 450 GeV) dump for the SPS accelerator. It must withstand the entire range of beams accelerated in the SPS supercycle, including fixed target experiments and injection into the LHC (see Table 1).

Table 1: SPS Run 2 Beam Energies and Intensities

Name	E [GeV]	Bunch Int.	# of Bunches
LHC 25 ns	450	1.2e11	288
LHC 50 ns	450	1.2e11	144
Doublet	450	1.6e11	144
Fixed Target	400	9.52e9	4200

The waveforms of 2 vertical kickers combined with 3 horizontal sweepers in the SPS beam dump system make the whole beam be spread over a relatively large area on the front face of the absorbing core. Since year 2000 three devices have been installed: TIDVG 1 (2000 – 2004), TIDVG 2, (2006 – 2013), TIDVG 3 (installed in 2014). The composition of the three TIDVGs is broadly similar. TIDVG 1 and 2 consist of an absorbing core, encased in a copper jacket surrounded by iron shielding, both containing cooling pipes. The absorbing core is composed of 2.5 m of graphite,

1.0 m of aluminium, 0.5 m of copper and 0.3 m of tungsten. TIDVG3 has a slightly longer (2.7 m) graphite section and a slightly shorter (0.8 m) Al section, because it is the limiting component [1]. During LS1, an endoscopy of TIDVG2 showed significant damage to the Al core section. Energy deposition and thermo-mechanical studies indicated that it did not come from one powerful shot but more likely repetitive dumping of a high power beam. TIDVG2 needed to be replaced by TIDVG3, reusing the iron yoke.

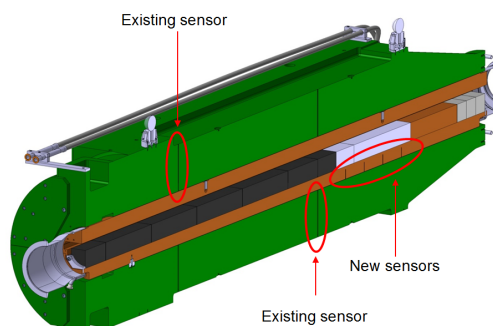


Figure 1: Position of existing and new temperature sensors in the yoke and copper jacket.

Four temperature sensors are installed in the yoke, positioned to give an indication of the temperature on the Cu jacket. Only 2 will be connected due to the number of available connections. Before installation 4 new sensors were inserted into the replacement Cu jacket, positioned to provide sufficient coverage as well as redundancy around the Al section (see Fig. 1). Finally, sensors were installed at the entrance and exit of one cooling circuits, in the Cu jacket.

The extent of the damage prompted several studies to determine the most likely time period when it occurred, and to develop an improved thermo-mechanical model. It serves as a post-mortem tool and to set operational limits for the TIDVG3 for future runs. This paper details the steps taken to improve and verify the simulation model.

## SIMULATIONS

### Energy Deposition Simulations

FLUKA [2, 3] simulations used a model of the TIDVG3 geometry, and particle density maps from tracking simulations as input (see Fig. 2). Energy density maps for each Run2 beam type are then used as input for the following thermo-mechanical studies. Fig. 3 shows the simulated peak energy deposition along the absorbing core of the TIDVG

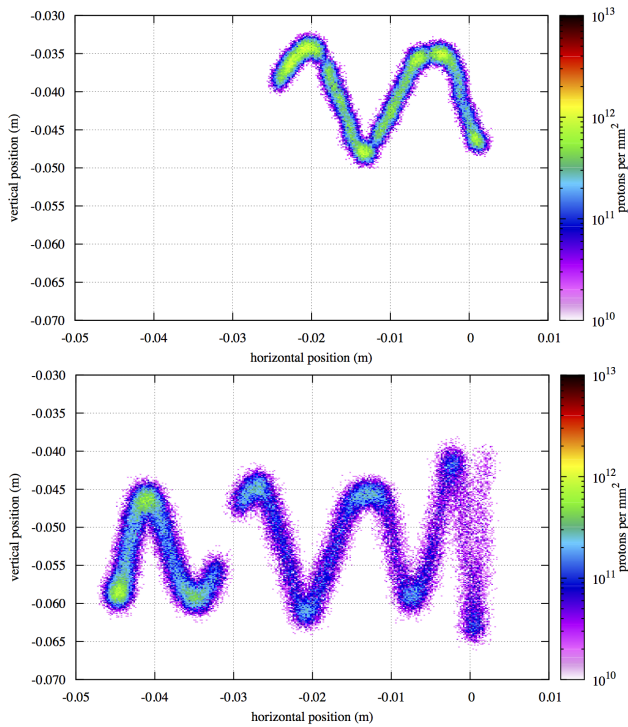


Figure 2: Impact distributions of SPS Run2 beams. Top: LHC 25 ns. Bottom: Fixed Target. LHC 50 ns is like the 25 ns sweep but with more obvious bunch separation. The doublet beam is like the right-hand arch of the LHC 25 ns.

for the 4 differing beam types. The peaks seen in the Al, Cu and W blocks for the two standard LHC beams and the doublet beam are dictated by the total beam intensity. The sweep of the fixed target beam covers a larger area: this is the dominating variable. This means that despite having the largest total number of protons, the power of the beam is deposited over a larger area, so peak values throughout the absorbing core are comparatively lower.

### Thermo-mechanical Simulations

Thermo-mechanical simulations performed using ANSYS [4] focus on the absorbing core and the Cu jacket since they absorb around 40% and 37% of the beam energy respectively,

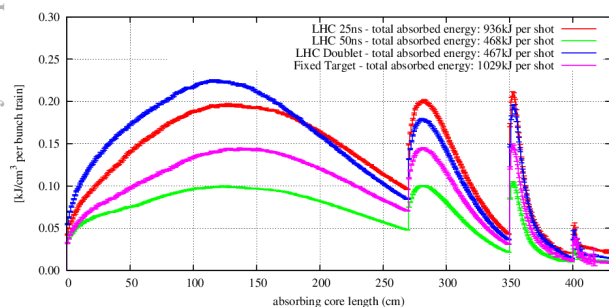


Figure 3: Peak energy density as a function of longitudinal position, for the 4 main Run 2 beam types. Total absorbed energy values given for the absorbing core.

compared to 13% for the iron cladding (with the remaining 10% escaping the device entirely). The effect of thermal radiation on the cooling was found to be negligible.

The absorbing core does not have any method of direct cooling, so the energy deposited in it is evacuated by the cooling pipes in the Cu jacket due to the contact between both. It is dependent on the Thermal Contact Conductance (TCC) between them. Two springs apply a force on the absorbing blocks, increasing the contact pressure and the TCC. During removal of one Al block of TIDVG3, imprints left by the springs in the material were observed. They reduced the compression of the springs, and the force applied on the blocks. For a design compression of 0.6 mm the respective load is 20 N/mm (the length dependence is due to the spring orientation in the device); the imprints reduced the compression to 0.32 mm, for a load of 10.7 N/mm.

The TCC is calculated using the Mikic model [5] for metal-to-metal contact and the Marotta model [6] for the graphite to copper boundaries. The effect of increased TTC with decreased heat exchange surface was assessed. Despite the higher pressures (and TCCs) for the smaller surface area cases and constant spring load, simulations showed a higher peak temperature: the smaller heat exchange surface is not compensated for by the increase in TCC. To ensure conservative conclusions, the minimum surface of heat exchange must be used. An uncoupled model is applied with conservative values for thermal and structural behaviour. Consequently the pressure profiles and their evolution during the heating due to beam impact and cooling cycles were investigated.

TIDVGs undergo a ‘bakeout’, the absorbing core heated to  $\sim 250^\circ\text{C}$  to accelerate the outgassing of the graphite; but it ‘ages’ the Al, diminishing its strength. Its total time was  $\sim 350$  h. Changes in the material properties were estimated from a similar Al alloy [7]. A temperature limit of  $250^\circ\text{C}$  was set for the Al blocks during repeated beam dumps, with no further degradation of the material properties predicted.

The simulations were performed for a variety of scenarios. Each of the 4 beam types of Table 1 was considered separately with the repetition rates of Table 2. A final 5th scenario was conceived to reflect a SPS supercycle: 1 pulse of LHC 25 ns; 15 s of cooling; 1 pulse of 5% of Fixed Target; 20 s of cooling; repeat previous until steady state is reached; once steady state is reached after pulse of LHC 25 ns, 6 s of cooling before 1 final pulse of 100% of Fixed Target.

Table 2: SPS Run 2 Beam Time Structure

Name	Bunch Spacing[s]	Pulse Duration[s]	Pulse Period[s]
LHC 25 ns	25.0e9	7.2e-6	21.6
LHC 50 ns	50.0e-9	7.2e-6	43.2
Doublet	25.0e-9	3.6e-6	43.2
Fixed Target	5.0e-9	21.0e-6	14.4

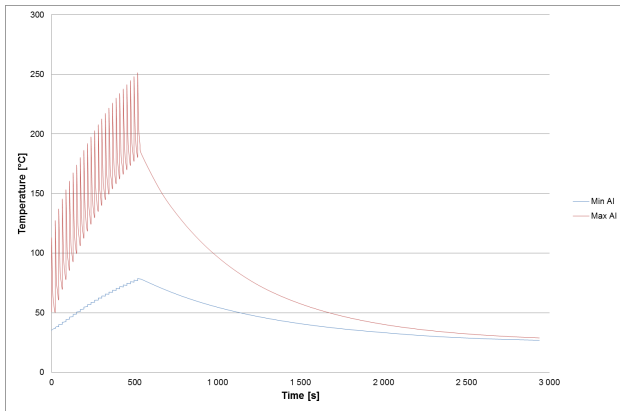


Figure 4: Peak (red) and minimum (blue) temperature in Al block during repeated dumping of LHC 25 ns beam, up to limit temperature, followed by cool down to original state.

**Results**

For LHC 25 ns beam the limit temperature in the Al block (250°C) is reached after 25 pulses, then 30 min are required to return back to the starting temperature of 35°C (see Fig. 4). If an additional 15 s of cooling time is added between each pulse, a steady state with a peak temperature below the limit is achieved. Both the LHC 50 ns and the doublet beams reach a steady state limit (at 121°C and 164°C respectively) without any cooling time between shots. Conversely, the fixed target beams are not dumped continuously, but are in the worst case in 3 series of 3 pulses spaced by 40 s. A steady state is not reached but the maximum temperature (205°C) is below the limit, taking 24 min to return to initial conditions.

For the 5th scenario, a steady state is reached with a peak temperature in Al of just under 250°C. Being only for a short period over a small volume of Al, this case is accepted. The temperature to be returned to (to allow for continued running in steady state) after a 100% fixed target beam impact is set to be 179°C. This is achieved 70 s after the impact, during which no more beam must be seen by the device.

**DATA - SIMULATION COMPARISONS**

The restart of the SPS after LS1 provided an opportunity to verify the simulations performed for the TIDVG, only for low intensity beams. Figure 5 top indicates that the simulated power transfer from the absorbing core to the cooling pipe is accurate. A similar agreement is seen for the iron shielding. However there is a difference for the Cu jacket surrounding the Al section (see Fig. 5 bottom). The TCC could be lower than in simulations, and a local peak temperature in the Al block higher than predicted. The difference is only a couple of degrees, but corresponds to ~ 50% when considering the  $\Delta T$  over the heating and cooling cycle. The return to high intensity beams will clarify if this is a statistical or not.

If the effect is non-statistical, it could be due to the flatness of the Cu jacket where it comes into contact with the absorbing core blocks. If this surface is bowed slightly the effective thermal exchange surface area is once again reduced. The

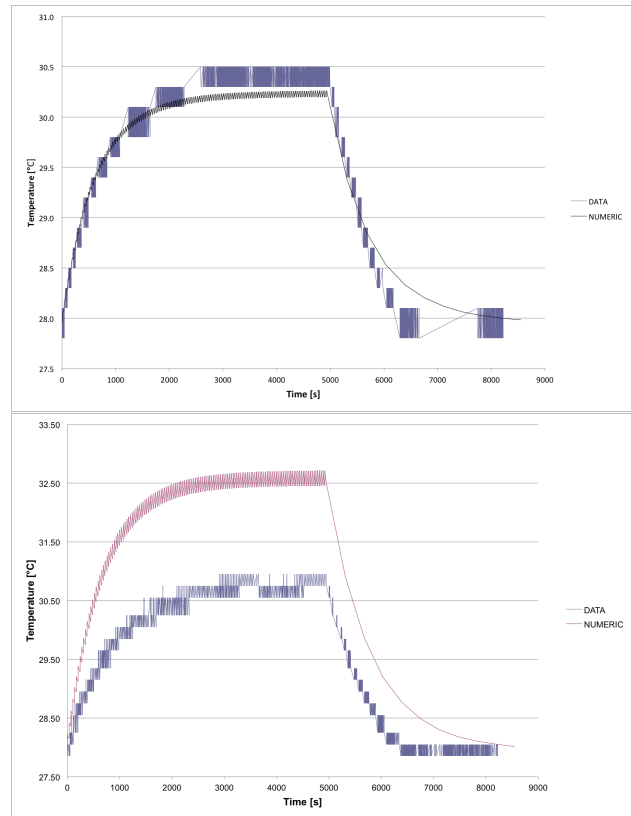


Figure 5: Comparison with measurement. Top: ANSYS simulated temperature (black); recorded data from TIDVG3 sensor (blue) for the exit of the Cu jacket water cooling system. Bottom: simulation (red); data (blue) for the Cu jacket near the Al section of the absorbing core.

Al-Cu contacts having a lower TCC due to the non-ideal flatness will correspond to Al sections with a higher peak temperature. If this is the case the model used for the results in this paper will no longer be conservative.

**CONCLUSIONS**

The simulation model used for the TIDVG has been carefully re-considered. As far as possible, where assumptions have to be made, they have been investigated to ensure that they are conservative. Early indications from the comparison of the results to data shows that the assumptions may still not be conservative enough. Continued data taking, with higher intensity beams should be performed to continue the verification of the improved model, and if necessary modify to produce new results. The aim of the study is to provide operational limits that will ensure the safe operation of the TIDVG 3 dump for the time being, however it is clear in the long term, the existing design is no longer suitable for the types of beams accelerated by the SPS. The demands on the SPS Internal dump system will become even more severe with the advent of the High Luminosity LHC, for which the SPS is part of the LHC Injectors Upgrade package.

## REFERENCES

- [1] O. Aberle. “Energy deposition and material resistance for LIU beams”, LIU-SPS Internal Beam Dump Review, January 2013.
- [2] T. T. Bohlen, F. Cerutti, M. P. W. Chin, A. Fassò, A. Ferrari, P. G. Ortega, A. Mairani, P. R. Sala, G. Smirnov, and V. Vlachoudis, “The FLUKA Code: Developments and Challenges for High Energy and Medical Applications”, Nuclear Data Sheets 120, 211-214 (2014).
- [3] A. Ferrari, P. R. Sala, A. Fassò and J. Ranft, “FLUKA: a multi-particle transport code”, CERN-2005-10 (2005), INFN/TC\_05/11, SLAC-R-773.
- [4] ANSYS®Academic Research, Release 15.0.
- [5] B. B. Mikic “Thermal contact conductance: theoretical considerations”, Int J Heat Mass Transfer 17:205–214 (1974).
- [6] E. Marotta, S. Mazzucca, J. Norley. “Thermal Joint Conductance for Graphite Materials”, Electronic Cooling, 8 (2003).
- [7] J. G. Kaufman. “Properties of Aluminium Alloys - Tensile, Creep and Fatigue Data at High and Low Temperatures”, ASM International, (1999).